Scientific Research Publishing

Modern Mechanical Engineering, 2018, 8, 121-139
http://www.scirp.org/journal/mme
ISSN Online: 2164-0181
ISSN Print: 2164-0165

An Underactuated Linkage Finger Mechanism for Hand Prostheses

H. M. C. M. Herath, R. A. R. C. Gopura, Thilina D. Lalitharatne

Bionics Laboratory, Department of Mechanical Engineering, University of Moratuwa, Katubedda, Sri Lanka
Email: gopurar@uom.lk

How to cite this paper: Herath, H.M.C.M., Gopura, R.A.R.C. and Lalitharatne, T.D. (2018) An Underactuated Linkage Finger Mechanism for Hand Prostheses. *Modern Mechanical Engineering*, **8**, 121-139.
https://doi.org/10.4236/mme.2018.82009

Received: January 20, 2018
Accepted: May 12, 2018
Published: May 15, 2018

Abstract

The underactuated fingers used in numerous robotic systems are evaluated by grasping force, configuration space, actuation method, precision of operation, compactness and weight. In consideration of all such factors a novel linkage based underactuated finger with a self-adaptive actuation mechanism is proposed to be used in prosthetics hands, where the finger can accomplish flexion and extension. Notably, the proposed mechanism can be characterized as a combination of parallel and series links. The mobility of the system has been analyzed according to the Chebychev-Grübler-Kutzbach criterion for a planar mechanism. With the intention of verifying the effectiveness of the mechanism, kinematics analysis has been carried out, by means of the geometric representation and Denavit-Hartenberg (D-H) parameter approach. The presented two-step analysis followed by a numerical study, eliminates the limitations of the D-H conversion method to analyze the robotics systems with both series and parallel links. In addition, the trajectories and configuration space of the proposed finger mechanism have been determined by the motion simulations. A prototype of the proposed finger mechanism has been fabricated using 3D printing and it has been experimentally tested to validate its functionality. The kinematic analysis, motion simulations, experimental investigations and finite element analysis have demonstrated the effectiveness of the proposed mechanism to gain the expected motions.

Keywords

Linkage Finger Mechanism, Underactuation, Kinematic Analysis, Denavit-Hartenberg Conversion, Geometric Representation

1. Introduction

Progressively, the researchers have developed different robotic fingers with various functionalities and mechanisms. Such robotic fingers are functional in var-

ious applications, for instance prosthetic hands, industrial grippers, surgical robots and scape robot arms. The effectiveness of an artificial finger will depend on its ability to apply an extensive range of grasping forces, generation of precise motion patterns and establishment of a comprehensive configuration space [1]. Furthermore, endurance to external loads while offering a compact and lightweight hardware will be advantageous [2].

Nearly, in the past three decades of period, numerous prosthetic finger mechanisms have been developed by the use of tendon-based mechanisms [3], crossed-bar mechanism [4], belt or gears based mechanisms [5] [6], wire driving methods using elastic elements [7], flexible fluidic actuators [8], torsion spring based mechanisms [9] [10] and linkage based mechanisms [11] [12]. Among all such mechanisms, the tendon driven, and linkage-based mechanisms have been presented a widespread in underactuated prosthetic finger developments. Significantly, the underactuated mechanisms have the capability to operate with less number of drivers than the degrees of freedom (DoF) of the mechanism [1], which will be beneficial to introduce compact and light weight designs. In consideration of tendon-based mechanisms, the tendon ropes are endure for limited tension and can be demonstrated elastic deformation, which may affect the performance of the finger. Therefore, the tendon-based underactuated mechanism is mostly suitable for the applications, which has comparatively a less workload, and finger contact force. [1] [13]. However, in order to achieve strong grasping forces it may have need of using larger actuators. Conversely, the larger actuators will take a higher actuation time. With the intention of overcoming all such issues, Phlernjai *et al.* have developed two-phase grasping mechanisms with the use of variable gear transmissions, where the fingers move in a high speed prior to contact with the object and a high force after the contact [2]. Most of the underactuated fingers are inherent with self-adaptive ability. In 2014, Li *et al.* have introduced an underactuated finger with first coupled and secondly self-adaptive grasping mode. Those fingers can adaptively grasp objects with different sizes and shapes while its motions during grasping are anthropopathic [14]. Moreover, Belzile *et al.* have been succeed in developing an optimal design of self-adaptive fingers for proprioceptive tactile sensing [15]. Fascinatingly, the variable stiffness robotic gripper introduced by Yang *et al.* is composed of two materials, acrylonitrile butadiene styrene for the bone segments and shape-memory polymer (SMP) for the finger joints. The SMP joints are exposed to thermal energy and heated above its glass transition temperature (Tg), where the finger joints exhibit very small stiffness bending by an external force. The finger will restore to its original shape due to SMP's shape recovering stress [16].

However, in consideration of power grasping applications with a high workload and finger contact force, such prosthetic hands have a need of powerful actuators to be placed inside the fingers, which will create an excessive weight, which should bear by the amputee. This research proposes a novel linkage based finger mechanism, which is mostly applicable for the grasping applications with a high workload and finger contact force. Besides, the proposed mechanism

cause to move by the cables, can be made with less in weight since there is no need to place any actuator inside the finger. Subsequently, a self-adaptive actuation method is presented.

In the last 150 years, several approaches have been proposed for the calculation of the mobility of the mechanisms. In the second half of the 19th century and the beginning of the 20th century the Chebychev-Grübler-Kutzbach criterion for multi-loop mechanisms were set up. Different versions of these formula were proposed all along the 20th century by Dobrovolski (1949-1951), Artobolevskii (1953) Kolchin (1960) Rössner (1961), Boden (1962), Ozol (1963), Manolescu and Manafu (1963), Bagci (1971), Hunt (1978), Tsai (1999) [17]. Significantly, the criterion can break down for mechanisms with special geometries and particularly for the over-constrained parallel mechanisms [18]. The Chebychev-Grübler-Kutzbach criterion explicit the relationship between the mobility and the structural parameters of the mechanism. Moreover, to accomplish precise and controlled motion patterns, the understanding of the kinematics is extremely essential. Chen *et al.* have presented the kinematic and dynamic characteristics of the human finger as a preliminary step towards the development of robotic and prosthetic fingers that imitate the human finger functions [19]. Several approaches have been deliberated by the researches, in order to analyze the kinematics of the diverse finger mechanisms. For instance, Licheng *et al.* have considered positional kinematics of the finger at different stages and the kinematic analysis of the equivalent mechanism of each stage has been carried out, for their fully rotational finger [1]. Furthermore, Screw theory has been used to establish the general kinematic both of series and parallel manipulators. With the aid of screw theory, Hunt *et al.* have shown that, a workpiece grasped by a fully-in-series manipulator can only lose freedom, while a workpiece grasped by a fully-in-parallel manipulator can only gain freedom [20]. According to the comparison carried out by Rocha *et al.*, the main feature of the screw-based kinematic modelling is the uniformity. In addition, screw-based modelling is advantageous in differential kinematics [21]. However, The Denavit-Hartenberg (D-H) approach is more popular and widely adopted in research than the Screw theory [22]-[27]. D-H conventions model has been originally applied into single loop chains but now almost universally applied to open loop serial chains [28].

The novel linkage mechanism presented in this paper can be identified as a combination of parallel and series links. Consequently, the mobility of the system has been analyzed according to Chebychev-Grübler-Kutzbach criterion for a planar mechanism. A combination of geometric relations and Denavit-Hartenberg conversion have been deliberated to analyze the forward kinematics of the proposed mechanism. In addition, the trajectories and configuration space of the proposed finger mechanism are presented. The fabricated prototype has been experimentally tested and the comparison between the experimental and simulation results are demonstrated. Furthermore, finite element analysis has been carried out to ensure the structural performance. As presented in a previous publication of ours, this particular finger design has been used to

develop a prosthetic hand for power grasping applications [29]. By comparing to the existing self-adaptive and underactuated finger mechanisms, which do perform different grasps such as cylindrical, hook, lateral pinch, tip pinch and palmar pinch, the proposed underactuated mechanism has the unique ability to accomplish self-adaptive power grasps with higher finger contact forces [4] [29] [30]. In addition to the prosthetics, the proposed finger mechanism can be used to develop robotic or hydraulic grippers for several other applications, *i.e.* manufacturing, surgeries, drones and space operations.

2. Underactuated Linkage Mechanism

Figure 1 illustrates the schematic diagram of the joints and the links of the linkage finger mechanism. Accordingly, the proposed finger mechanism consists of proximal phalanx, intermediate phalanx and distal phalanx which are made of eleven different links. The metacarpophalangeal (MCP) joint of the finger denoted by point "A" will not be actuated. However the proximal interphalangeal (PIP) joint denoted by point "B", and distal interphalangeal (DIP) joint denoted by point "H" are designed to be set in rotary motion by any linear actuator, based on active or passive dynamics. The links PPT1, PPT2, PPM, PPB1, PPB2 are placed in the proximal phalanx and IPT1, IPT2, IPM, IPB1, IPB2 are placed in the intermediate phalanx. The link DP act as the distal phalanx. Besides, the rotary joints of the linkage mechanism are pointed out by "C", "E", "D", "B", "F", "G", "H" and "I". In addition, there are prismatic joints in between C-D, E-F, D-G, and F-I. Accordingly, AB, BH, HJ, CE, DF, GI, LK, GK and IL are fixed lengths where CD, EF, DG and FI are varying lengths. The linear motion of PPB2 towards PPB1, reduces the distance between C-D, which originates a counterclockwise (CCW) rotation on IPM around point "B" (PIP joint). This causes, PPT2 to move away from PPT1 and increase the distance between E-F. Similar way, the linear motion of IPB2 towards IPB1, originates a CWW rotation on DP around point "H" (DIP joint). These CCW rotations result for finger flexion. Contrariwise, the linear motions, PPT2 towards PPT1 and IPT2 towards IPT1, originate clockwise (CW) rotations on IPM and DP around PIP and DIP joints respectively. These CW rotations result for finger extension.

Prototype Finger and Actuation Method

The linkage mechanism explicated in the previous paragraph has been progressively applied to develop a prototype finger. Figure 2 illustrates design of the prototype finger. For the mechanical design, the anthropometric data of the Sri Lankan population has been considered, which were presented by Abeysekera *et al.* [31]. Intended for finger actuation, nylon strings are threaded through the holes in the bottom of the proximal phalanges (PPB1 and PPB2) then through the holes across the bottom of the Intermediate phalange (IPB1 and IPB2). Subsequently, those strings are tightly tied around using a knot and two pairs of small long nose plier are used to ensure the knot is tight. High-tension fiber cables such as carbon fiber can replace these nylons strings in order to contend

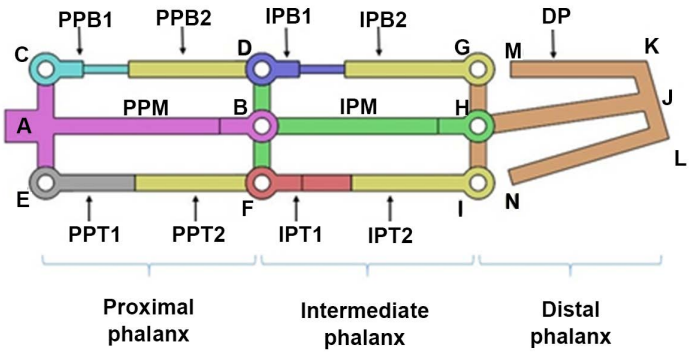

Figure 1. Links and joints of the linkage finger mechanism.

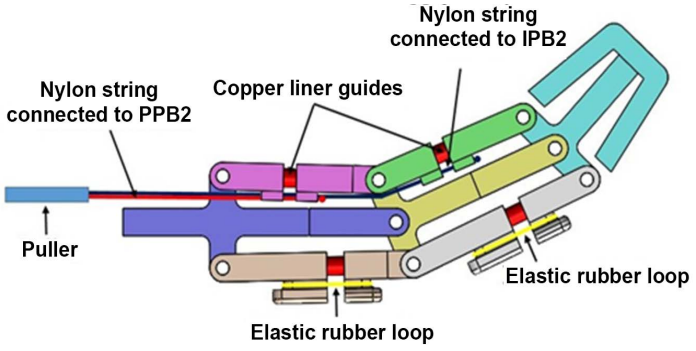

Figure 2. Design of the prototype finger.

with higher workloads. Elastic rubber loops are placed between PPT1 and PPT2, IPT1 and IPT2. Those rubber loops act as springs to obtain the reverse actuation and bring the finger the initial position. Figure 3 presents the fabricated prototype of the finger.

Furthermore, a simple hypothesis is proposed, in order to achieve self-adaptive grasping. Figure 4 illustrate the schematic representation of the proposed mechanism. As shown in the Figure 4, there are two pulleys and one end of the nylon string which goes around pulley A is connected to PPB2, where the other end is connected to IPB2. Similarly, the string which goes around pulley B is also connected to PPB2 and IPB2. As there are, two pulleys the forces are equally distributed among the both and it, benefits to reduce the lateral motions. Once the linear actuator generate a motion in the directions shown by arrows, the PIP and DIP joints are supposed to be adjusted adaptively to grasp the object.

3. Kinematics of the Finger

The kinematic analysis is essential to yield the improved performance of the mechanical design and to develop appropriate control algorithms. The full kinematic structure of the proposed prosthesis is shown in Figure 5(a). Altogether, there are eleven links and twelve joints. The consideration of the mobility is an important design criterion. However, mobility criteria are not applicable for most parallel robots [17]. Intended for analysis the mobility, the kinematic

Figure 3. Fabricated prototype of the linkage finger mechanism.

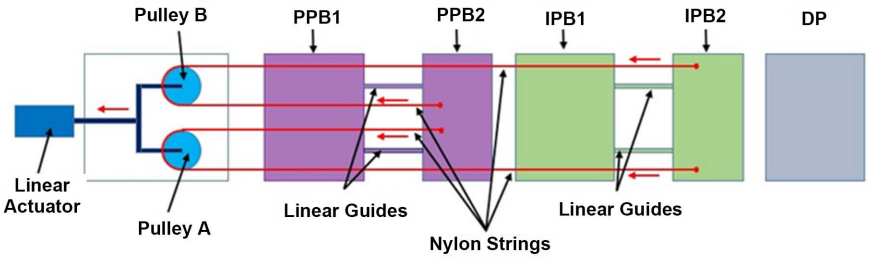

Figure 4. Proposed actuation method to accomplish self-adaptive grasps.

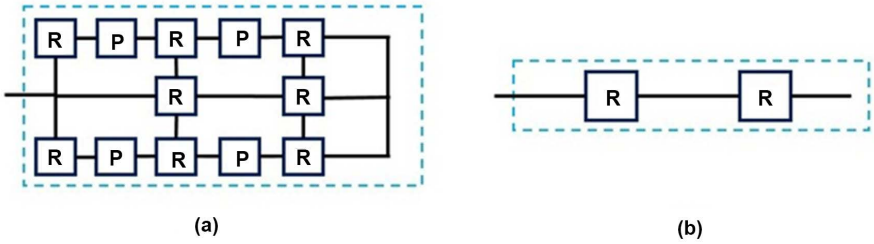

Figure 5. (a) Kinematic structure of the prosthetic finger; (b) Simplified kinematic structure for the mobility analysis.

representation of the finger mechanism has been simplified by assuming the middle links act as the bones, where the outer links act as muscles. **Figure 5(b)** illustrates the simplified kinematic structure for the mobility analysis. By means of the Chebychev-Grübler-Kutzbach criterion for a planar mechanism, the degree of freedom (DoF) of the proposed linkage mechanism has been determined by Equation (1).

$$F = 3(n - j - 1) + \sum_{i=1}^{j} f_i \tag{1}$$

where n is the number of links, j is the number of kinematic pairs and f_i is DoF of the i^{th} pair. For the simplified configuration without length varying links n equals 3, j equals 2 and Σf_i equals 2. Therefore, the effective DoF of the mechanism is equal to 2. Therefore, without considering the motions of the length varying links which represent muscles, the mechanism is capable of generating only two-motion configuration with a fixed set of joint angles. Furthermore, kinematic analysis of the mechanism has been carried out in two steps. In the first phase, the geometric representation has been depicted with the intention to initiate the relationships between the joint angles and the link

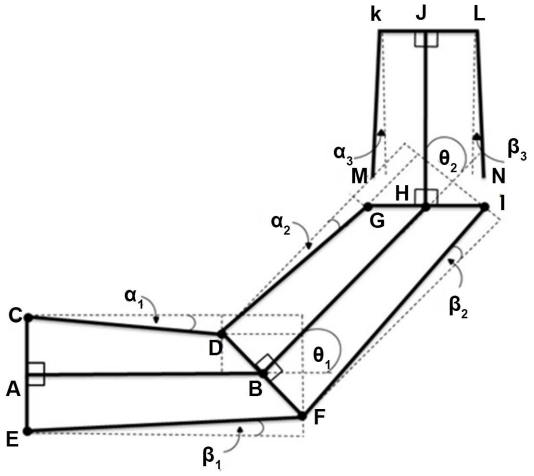

Figure 6. Geometric representation of the linkage finger mechanism.

lengths. Subsequently, in the second phase, the forward kinematic analysis has been carried out by means of Denavit-Hartenberg (D-H) approach, to determine the positions of the critical points on the finger with respect to the different CD and DG distances.

3.1. Geometric Representation

Figure 6 illustrates the geometric representation for the proposed underactuated finger mechanism. Accordingly, the PIP joint angle is $180 - \theta_1$ and DIP joint angle is $180 - \theta_2$. Rotation angles of the links CD, EF, DG and FI are represented by α_1, β_1, α_2 and β_2 respectively.

According to the geometry, following distances are equal.

$$AC = AE = BD = BF = GH = HI \tag{2}$$

Let us consider the links of the proximal phalanx. According the geometry,

$$EF\cos\beta_1 - AB = BF\sin\theta_1 \tag{3}$$

$$AB - CD\cos\alpha_1 = BD\sin\theta_1 \tag{4}$$

By considering, Equation (2), (3) and (4) it can be derived that,

$$2AB = EF\cos\beta_1 + CD\cos\alpha_1 \tag{5}$$

Moreover, according to the geometry it can be established that,

$$AC = BD\cos\theta_1 + CD\sin\alpha_1 \tag{6}$$

$$AE = BF\cos\theta_1 + EF\sin\beta_1 \tag{7}$$

By considering, Equation (2), (6) and (7) it can be derived that,

$$CD\sin\alpha_1 = EF\sin\beta_1 \tag{8}$$

According to the Pythagorean theorem,

$$CD = \sqrt{\left(AB - BD\sin\theta_1\right)^2 + \left(AC - BD\cos\theta_1\right)^2} \tag{9}$$

By considering the general principles of trigonometry and algebra, Equation

(9) can be simplified as,

$$\frac{CD^2 - AB^2 - AC^2 - BD^2}{-2BD} = AB\sin\theta_1 + AC\cos\theta_1 \tag{10}$$

According to trigonometry it can be derived that,

$$(AB)\sin\theta_1 + (AC)\cos\theta_1 = C_1\sin(\theta_1 + \delta_1) \tag{11}$$

where;

$$C_1 = \pm\sqrt{AB^2 + AC^2} \tag{12}$$

$$\delta_1 = \tan^{-1}\left(\frac{AC}{AB}\right) \tag{13}$$

By substituting to the right hand side of the Equation (10), from Equation (11), (12) and (13),

$$\frac{CD^2 - AB^2 - AC^2 - BD^2}{-2BD} = \pm\sqrt{AB^2 + AC^2}\left(\sin\left(\theta_1 + \left(\tan^{-1}\left(\frac{AC}{AB}\right)\right)\right)\right) \tag{14}$$

Equation (14) can simplified as below to establish a relationship between the angle θ_1 and the link lengths.

$$\theta_1 = \sin^{-1}\left(\frac{CD^2 - AB^2 - AC^2 - BD^2}{-2BD\left(\pm\sqrt{AB^2 + AC^2}\right)}\right) - \left(\tan^{-1}\left(\frac{AC}{AB}\right)\right) \tag{15}$$

$$\theta_1 = \sin^{-1}(A_1) - \delta_1 \tag{16}$$

where;

$$A_1 = \frac{CD^2 - AB^2 - AC^2 - BD^2}{-2BD\left(\pm\sqrt{AB^2 + AC^2}\right)} \tag{17}$$

$$\delta_1 = \tan^{-1}\left(\frac{AC}{AB}\right) \tag{18}$$

According to the Pythagorean theorem it can be derived that,

$$EF = \sqrt{(AB + BF\sin\theta_1)^2 + (AE - BF\cos\theta_1)^2} \tag{19}$$

By substituting the θ_1 from Equation (16), the Equation (19) can be written as,

$$EF = \sqrt{\left(AB + BF\sin\left(\sin^{-1}(A_1) - \delta_1\right)\right)^2 + \left(AE - BF\cos\left(\sin^{-1}(A_1) - \delta_1\right)\right)^2} \tag{20}$$

By substituting the θ_1 from Equation (16), the Equation (6) can be written as,

$$AC = BD\cos\left(\sin^{-1}(A_1) - \delta_1\right) + CD\sin\alpha_1 \tag{21}$$

Equation (21) can simplified as below to establish a relationship between the angle α_1 and the link lengths.

$$\alpha_1 = \sin^{-1}\frac{AC - BD\cos\left(\sin^{-1}(A_1) - \delta_1\right)}{CD} \tag{22}$$

By substituting the θ_1 from Equation (16), the Equation (7) can be written as,

$$AE = BF\cos\left(\sin^{-1}\left(A_1\right)-\delta_1\right)+EF\sin\beta_1 \tag{23}$$

By substituting EF from Equation (20), the Equation (23) can simplified as below to establish a relationship between the angle β_1 and the link lengths.

$$\beta_1 = \sin^{-1}\frac{AE - BF\cos\left(\sin^{-1}\left(A_1\right)-\delta_1\right)}{\sqrt{\left(AB+BF\sin\left(\sin^{-1}\left(A_1\right)-\delta_1\right)\right)^2+\left(AE-BF\cos\left(\sin^{-1}\left(A_1\right)-\delta_1\right)\right)^2}} \tag{24}$$

In the same way by considering the links in the intermediate phalanx, it can be proved that the relationship between the angle θ_2 and the link lengths are given by,

$$\theta_2 = \sin^{-1}\left(\frac{DG^2-BH^2-BD^2-GH^2}{-2GH\left(\pm\sqrt{BH^2+BD^2}\right)}\right)-\left(\tan^{-1}\left(\frac{BD}{BH}\right)\right) \tag{25}$$

$$\theta_2 = \sin^{-1}\left(A_2\right)-\delta_2 \tag{26}$$

where;

$$A_2 = \frac{DG^2-BH^2-BD^2-GH^2}{-2GH\left(\pm\sqrt{BH^2+BD^2}\right)} \tag{27}$$

$$\delta_2 = \tan^{-1}\left(\frac{BD}{BH}\right) \tag{28}$$

Furthermore, the relationship between the angle α_2 and the link lengths are given by,

$$\alpha_2 = \sin^{-1}\frac{BD-GH\cos\left(\sin^{-1}\left(A_2\right)-\delta_2\right)}{DG} \tag{29}$$

The relationship between the angle β_2 and the link lengths are given by,

$$\beta_2 = \sin^{-1}\frac{BF-HI\cos\left(\sin^{-1}\left(A_2\right)-\delta_2\right)}{\sqrt{\left(BH+HI\sin\left(\sin^{-1}\left(A_2\right)-\delta_2\right)\right)^2+\left(BF-HI\cos\left(\sin^{-1}\left(A_2\right)-\delta_2\right)\right)^2}} \tag{30}$$

3.2. Forward Kinematics

The forward kinematic analysis has been carried out by means of the Denavit-Hartenberg (DH) parameter approach. According to the D-H procedure described by the Rocha *et al.* [19], first the links and joints should be identified. Links and joints can be numbered from 0 to n. Subsequently, it is required to define the reference frames for the internal links. Then the reference frames should be defined for the extremities links. Successively, the D-H parameters for each link should be identified, where a_i is the distance between $z_i - 1$ and z_i. d_i is the distance between $x_i - 1$ and x_i. α_i is the angle between $z_i - 1$ and z_i measured along x_i, while θ_i is the angle between $x_i - 1$ and x_i measured along z_i. Then the homogeneous transformation matrices for each joint should be determined and finally the overall homogeneous transformation matrix by premultiplication of

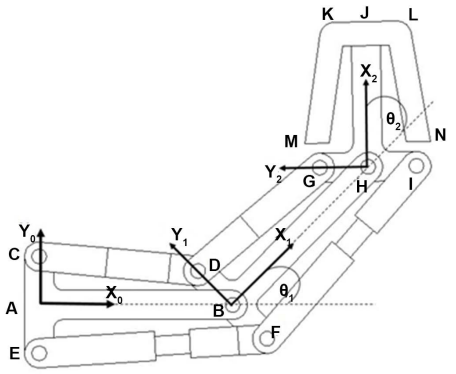

Figure 7. Link frame assignment of the linkage finger mechanism for Denavit-Hartenberg analysis.

Table 1. Denavit-Hartenberg link parameters.

Link No.	D-H Parameter			
	$\alpha_{(i-1)}$ (degrees)	$a_{(i-1)}$ (mm)	d_i (mm)	θ_i (degrees)
0	0	0	0	0
1	0	AB	0	θ_1
2	0	BH	0	θ_2

the individual joint transformation matrices should be determined. Accordingly, Figure 7 illustrates the link frame assignment of the linkage finger mechanism and Table 1 defines the Denavit-Hartenberg link parameters.

By referring to the link frame assignment and D-H link parameters. The rotation around the Z_0 axis can be denoted by,

$$ {}_0T = \begin{bmatrix} \cos 0 & -\sin 0 & 0 & 0 \\ (\sin 0)(\cos 0) & (\cos 0)(\cos 0) & -\sin 0 & (-\sin 0)(0) \\ (\sin 0)(\sin 0) & (\cos 0)(\sin 0) & \cos 0 & (\cos 0)(0) \\ 0 & 0 & 0 & 1 \end{bmatrix} \tag{31} $$

$$ {}_0T = \begin{bmatrix} 1 & 0 & 0 & 0 \\ 0 & 1 & 0 & 0 \\ 0 & 0 & 1 & 0 \\ 0 & 0 & 0 & 1 \end{bmatrix} \tag{32} $$

Subsequently, the translation by AB, followed by a rotation around the Z_1 axis, can be denoted by,

$$ {}^0_1T = \begin{bmatrix} \cos\theta_1 & -\sin\theta_1 & 0 & AB \\ (\sin\theta_1)(\cos 0) & (\cos\theta_1)(\cos 0) & -\sin 0 & (-\sin 0)(0) \\ (\sin\theta_1)(\sin 0) & (\cos\theta_1)(\sin 0) & \cos 0 & (\cos 0)(0) \\ 0 & 0 & 0 & 1 \end{bmatrix} \tag{33} $$

$$ {}^0_1T = \begin{bmatrix} \cos\theta_1 & -\sin\theta_1 & 0 & AB \\ \sin\theta_1 & \cos\theta_1 & 0 & 0 \\ 0 & 0 & 1 & 0 \\ 0 & 0 & 0 & 1 \end{bmatrix} \tag{34} $$

Successively, the translation by BH, followed by a rotation around the Z_2 axis, can be denoted by,

$$ {}^{1}_{2}T = \begin{bmatrix} \cos\theta_2 & -\sin\theta_2 & 0 & BH \\ (\sin\theta_2)(\cos 0) & (\cos\theta_2)(\cos 0) & -\sin 0 & (-\sin 0)(0) \\ (\sin\theta_2)(\sin 0) & (\cos\theta_2)(\sin 0) & \cos 0 & (\cos 0)(0) \\ 0 & 0 & 0 & 1 \end{bmatrix} \tag{35} $$

$$ {}^{1}_{2}T = \begin{bmatrix} \cos\theta_2 & -\sin\theta_2 & 0 & BH \\ \sin\theta_2 & \cos\theta_2 & 0 & 0 \\ 0 & 0 & 1 & 0 \\ 0 & 0 & 0 & 1 \end{bmatrix} \tag{36} $$

According to the Denavit-Hartenberg convention,

$$ {}^{0}_{2}T = \left({}_{0}T\right)\left({}^{0}_{1}T\right)\left({}^{1}_{2}T\right) \tag{37} $$

By substituting from the Equation (32), (34) and (36), the Equation (37) can be written as,

$$ {}^{0}_{2}T = \begin{bmatrix} 1 & 0 & 0 & 0 \\ 0 & 1 & 0 & 0 \\ 0 & 0 & 1 & 0 \\ 0 & 0 & 0 & 1 \end{bmatrix} \begin{bmatrix} \cos\theta_1 & -\sin\theta_1 & 0 & AB \\ \sin\theta_1 & \cos\theta_1 & 0 & 0 \\ 0 & 0 & 1 & 0 \\ 0 & 0 & 0 & 1 \end{bmatrix} \begin{bmatrix} \cos\theta_2 & -\sin\theta_2 & 0 & BH \\ \sin\theta_2 & \cos\theta_2 & 0 & 0 \\ 0 & 0 & 1 & 0 \\ 0 & 0 & 0 & 1 \end{bmatrix} \tag{38} $$

Subsequently, the Equation (38) can be simplified as below,

$$ {}^{0}_{2}T = \begin{bmatrix} \cos(\theta_1+\theta_2) & -\sin(\theta_1+\theta_2) & 0 & BH\cos\theta_1 + AB \\ \sin(\theta_1+\theta_2) & \cos(\theta_1+\theta_2) & 0 & BH\sin\theta_1 \\ 0 & 0 & 1 & 0 \\ 0 & 0 & 0 & 1 \end{bmatrix} \tag{39} $$

The position of the point D with respect to the origin can be defined as,

$$ D^{x_0y_0z_0} = {}^{0}_{1}T \begin{bmatrix} D^{x_1} \\ D^{y_1} \\ D^{z_1} \\ 1 \end{bmatrix} \tag{40} $$

where,

$$ \begin{bmatrix} D^{x_1} \\ D^{y_1} \\ D^{z_1} \\ 1 \end{bmatrix} = \begin{bmatrix} 0 \\ BD \\ 0 \\ 1 \end{bmatrix} \tag{41} $$

Substituting from Equation (34) and (41), the Equation (40) can be written as,

$$ D^{x_0y_0z_0} = \begin{bmatrix} \cos\theta_1 & -\sin\theta_1 & 0 & AB \\ \sin\theta_1 & \cos\theta_1 & 0 & 0 \\ 0 & 0 & 1 & 0 \\ 0 & 0 & 0 & 1 \end{bmatrix} \begin{bmatrix} 0 \\ BD \\ 0 \\ 1 \end{bmatrix} \tag{42} $$

Furthermore, the Equation (42) can be simplified as below to describe the po-

sition of the point D with respect to the origin.

$$D^{x_0y_0z_0} = \begin{bmatrix} -BD\sin\theta_1 + AB \\ BD\cos\theta_1 \\ 0 \\ 1 \end{bmatrix} \tag{43}$$

Likewise, the position of the point G with respect to the origin can be defined as,

$$G^{x_0y_0z_0} = {}^0_2T \begin{bmatrix} G^{x_2} \\ G^{y_2} \\ G^{z_2} \\ 1 \end{bmatrix} \tag{44}$$

where,

$$\begin{bmatrix} G^{x_2} \\ G^{y_2} \\ G^{z_2} \\ 1 \end{bmatrix} = \begin{bmatrix} 0 \\ GH \\ 0 \\ 1 \end{bmatrix} \tag{45}$$

Substituting from Equation (36) and (45), the Equation (44) can be written as,

$$G^{x_0y_0z_0} = \begin{bmatrix} \cos(\theta_1+\theta_2) & -\sin(\theta_1+\theta_2) & 0 & BH\cos\theta_1 + AB \\ \sin(\theta_1+\theta_2) & \cos(\theta_1+\theta_2) & 0 & BH\sin\theta_1 \\ 0 & 0 & 1 & 0 \\ 0 & 0 & 0 & 1 \end{bmatrix} \begin{bmatrix} 0 \\ GH \\ 0 \\ 1 \end{bmatrix} \tag{46}$$

Afterwards the Equation (46) can be simplified as below to describe the position of the point G with respect to the origin.

$$G^{x_0y_0z_0} = \begin{bmatrix} -GH\sin(\theta_1+\theta_2) + BH\cos\theta_1 + AB \\ GH\cos(\theta_1+\theta_2) + BH\sin\theta_1 \\ 0 \\ 1 \end{bmatrix} \tag{47}$$

Successively, the position of the point K with respect to the origin can be defined as,

$$K^{x_0y_0z_0} = {}^0_2T \begin{bmatrix} K^{x_2} \\ K^{y_2} \\ K^{z_2} \\ 1 \end{bmatrix} \tag{48}$$

where,

$$\begin{bmatrix} K^{x_2} \\ K^{y_2} \\ K^{z_2} \\ 1 \end{bmatrix} = \begin{bmatrix} HJ \\ JK \\ 0 \\ 1 \end{bmatrix} \tag{49}$$

Substituting from Equation (39) and (49), the Equation (48) can be written as,

$$K^{x_0y_0z_0} = \begin{bmatrix} \cos(\theta_1+\theta_2) & -\sin(\theta_1+\theta_2) & 0 & BH\cos\theta_1 + AB \\ \sin(\theta_1+\theta_2) & \cos(\theta_1+\theta_2) & 0 & BH\sin\theta_1 \\ 0 & 0 & 1 & 0 \\ 0 & 0 & 0 & 1 \end{bmatrix} \begin{bmatrix} HJ \\ JK \\ 0 \\ 1 \end{bmatrix} \quad (50)$$

Furthermore, the Equation (50) can be simplified as below to describe the position of the point K with respect to the origin.

$$K^{x_0y_0z_0} = \begin{bmatrix} HJ\cos(\theta_1+\theta_2) - JK\sin(\theta_1+\theta_2)) + BH\cos\theta_1 + AB \\ HJ\sin(\theta_1+\theta_2) + JK\cos(\theta_1+\theta_2) + BH\sin\theta_1 \\ 0 \\ 1 \end{bmatrix} \quad (51)$$

4. Analysis and Results

The prototype of the linkage finger mechanism has been designed with the link parameters demonstrated in Table 2. By considering the link parameter values and referring to the kinematic analysis, a MatLab program has been developed to plot the positions of the points D, G and K, with respect to the different CD and DG distances. By substituting the values for θ_1 and θ_2 from Equation (16) and (26) to Equation (43), (47) and (51) the X and Y coordinates of the points D, G and K have been plotted as illustrated in Figure 8. Furthermore, by substituting link lengths values for the Equation (16) and (26), it has been identified that, during the maximum flexion of the finger, both PIP and DIP joint angles are equal to 134.5˚ where CD and DG distances are at its minimum of 33 mm. Contrariwise, once the CD and DG equals to 40 mm the finger achieve its maximum extension where PIP and DIP joint angles are equal to 180˚. The configuration space of a finger is its range of movement. A finger can only perform within the confines of this configuration space. As shown in Figure 9, the finger trajectories and the configuration space of the proposed finger in X-Y coordinate system (origin is at MCP joint) has been determined by using the motions simulations inbuilt with Solidworks software package. Based on the finger trajectories and the configuration space, different prosthetic terminal devices can be developed, in order to accomplish the anticipated grasps patterns.

Furthermore, experimental investigations have been carried out to confirm the motions of the proposed finger mechanism. Accordingly, the sequence of the finger motions throughout the actuation of the prototype were captured by using a digital camera, as presented in Figure 10. Subsequently, by using the ImageJ open source image processing software package [32], the DIP and PIP joint

Table 2. Link parameter values for the prototype finger.

Parameter	Constant				Variable	
	AC, AE, BD, BF, GH, HI	AB, BH	HJ	LJ, JK	CD, DG	EF, FI
Length (mm)	10	40	30	9	33 to 40	40 to 47

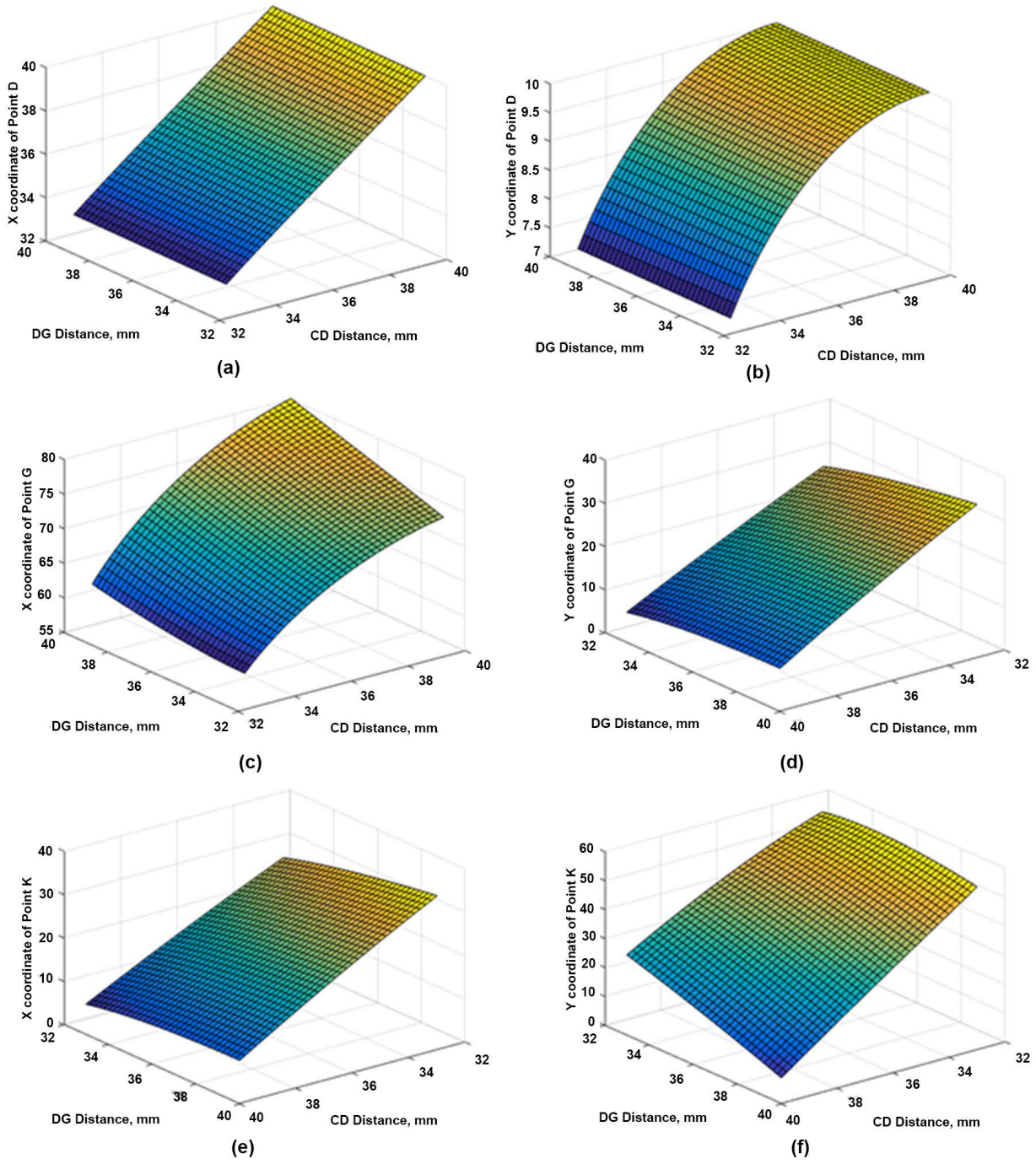

Figure 8. X and Y coordinates of the different finger positions with respect to the CD and DG distance (a) X coordinate of Point D; (b) Y coordinate of Point D; (c) X coordinate of Point G; (d) Y coordinate of Point G; (e) X coordinate of Point K; (f) Y coordinate of Point K.

angles of the prototype were measured with respect to different CD and DG distances. As presented in **Figure 11**, the experimental results have been compared with the simulations. There is a difference (up to two degrees) between the experimental and simulation results. The backlash of the links due to less precision of fabrication and the instabilities of the camera might have caused such errors.

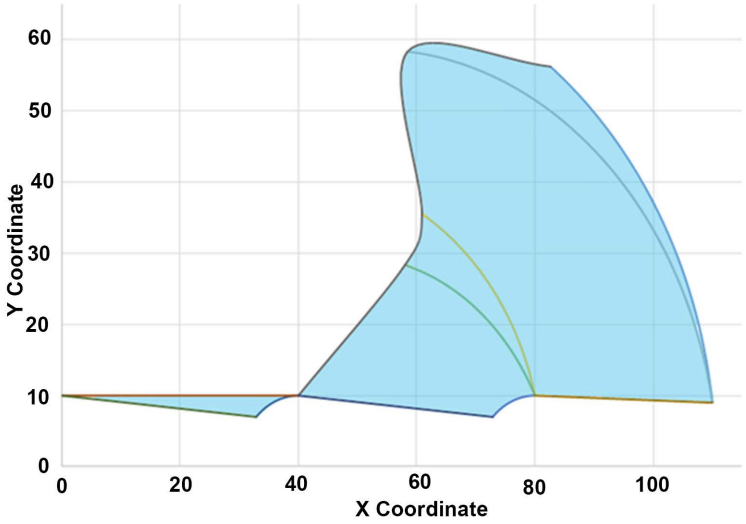

Figure 9. Trajectories and the configuration space of the linkage finger mechanism.

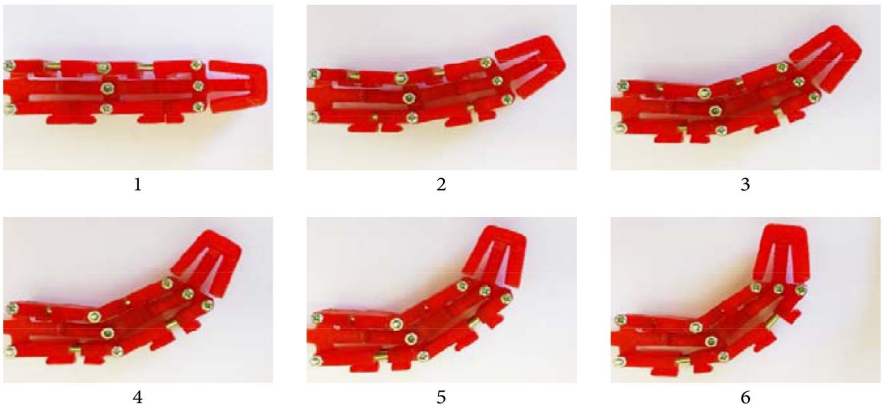

Figure 10. Sequence of the finger motions with respect to change of both CD and DG distances.

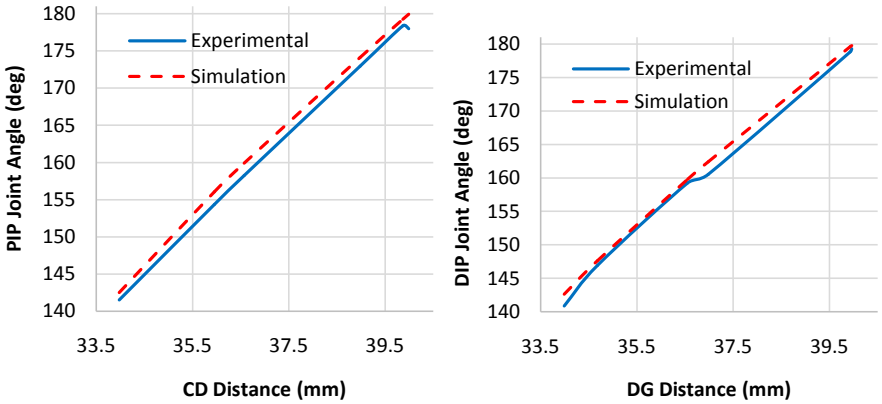

Figure 11. Comparison between the experimental measurements and motion simulation results for link lengths and joint angles (a) PIP joint angle against CD distance; (b) DIP joint angle against DG distance.

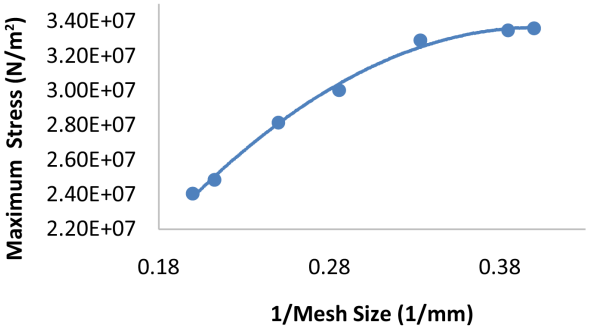

Figure 12. Convergence of the finite element analysis.

The finite element analysis (FEA) by Solidworks simulations proved that the finger is sturdy to withstand the standard finger forces. Designed prosthetic finger mechanism is expected to carry 20 N payload at distal phalanx. In addition to the play load it is assumed that 5 N is applied by the elastics rubber loops as a spring effect. Further the tension of nylon strings has been is taken as 10 N where it applies a pull on PPB2 and IPB2. Von misses stress, resultant displacement and equivalent strain of the finger have been determined by FEA. According to the results, the designed finger has a maximum von Mises Stress of 3.36e+007 N/m^2, maximum resultant displacement of 1.55 mm and maximum equivalent strain of 0.008 where the Yield strength, Tensile strength and Elastic modulus of the material (PLA) are 7e+007 N/m^2, 7.3e+007 N/m^2, 3.5e+009 N/m^2 respectively. The minimum factor of safety has been determined as 2. The convergence analysis has been carried out for randomly chosen mesh sizes and the results are presented in Figure 12. According to the polynomial curve, the results are converging.

5. Conclusion

This paper proposes a novel underactuated linkage finger mechanism, which is a combination of series and parallel links. Although the Chebychev-Grübler-Kutzbach criterion has limitations to analyze parallel robots, the simplification of the kinematic representation has been applicable to analyze the mobility of the proposed linkage mechanism. However, it was only able to demonstrate the effective DoF for finger grasps and was unable to demonstrate a clear understanding on friction of the mechanism. Even though the mobility analysis proposed that the mechanism has two DoF, the finger can be actuated by a single linear actuator. Hence, the presented linkage finger mechanism is competent as an underactuated mechanism. Furthermore, the proposed mechanism can be developed, without placing any actuators inside the finger, thus lightweight prosthetic devices can be introduced to accomplish grasps with high workload and finger contact forces. The explicated two-step kinematic analysis, first generating the relationships between the link lengths and the joint angles, then D-H conversion towards the forward kinematics is an impeccable approach to analyze

the systems, which are developed as a hybrid of series and parallel links. Furthermore, the experimental investigation has verified the functionality of the finger and the exactitude of the analysis carried out. The outcomes of the kinematic analysis, establishment of the trajectories and the configuration space for the proposed mechanism, will be beneficial for future research towards developing control algorithms for the finger actuation.

Acknowledgements

The authors are indebted to the Department of Mechanical and Manufacturing Engineering, University of Ruhuna, Sri Lanka, for providing the fabrication facilities.

References

[1] Wu, L.C., Kong, Y.X. and Li, X.L. (2016) A Fully Rotational Joint Underactuated Finger Mechanism and its Kinematics Analysis. *International Journal of Advanced Robotic Systems*, **13**, 1-9. https://doi.org/10.1177/1729881416663373

[2] Phlernjai, M., Takayama, T. and Omata, T. (2016) Passively Switched Cable-Driven Transmission for High-Speed/High-Force Robot Finger. *Advanced Robotics*, **30**, 1559-1570. https://doi.org/10.1080/01691864.2016.1251336

[3] Rossi, C. and Savino, S. (2013) Mechanical Model of A Single Tendon Finger. *AIP Conference Proceedings*, **1558**, 1286-1292. https://doi.org/10.1063/1.4825746

[4] Bandara, D.S.V., Gopura, R.A.R.C., Brunthavan, G.K.M. and Abeynayake, H.I.M.M. (2014) An Under-Actuated Mechanism for A Robotic Finger. *Proceedings of the 4th Annual IEEE International Conference on Cyber Technology in Automation Control and Intelligent Systems*, Hong Kong, 407-412. https://doi.org/10.1109/CYBER.2014.6917498

[5] Liu, H., Meusel, P., Hirzinger, G., Jin, M., Liu, Y. and Xie, Z. (2008) The Modular Multisensory DLR-HIT-Hand: Hardware and Software Architecture. *IEEE/ASME Transactions on Mechatronics*, **13**, 461-469. https://doi.org/10.1109/TMECH.2008.2000826

[6] Koganezawa, K. and Ishizuka, Y. (2008) Novel Mechanism of Artificial Finger Using Double Planetary Gear System. *Proceedings of the* 2008 *IEEE/RSJ International Conference on Intelligent Robots and Systems*, Nice, 3184-3191. https://doi.org/10.1109/IROS.2008.4650589

[7] Kamikawa, Y. and Maeno, T. (2008) Underactuated Five-Finger Prosthetic Hand Inspired by Grasping Force Distribution of Humans. *Proceedings of the* 2008 *IEEE/RSJ International Conference on Intelligent Robots and Systems*, Nice, 717-722. https://doi.org/10.1109/IROS.2008.4650628

[8] Gaiser, I.N., Pylatiuk, C., Schulz, S., Kargov, A., Oberle, R. and Werner, T. (2009) The FLUIDHAND III: A Multifunctional Prosthetic Hand. *Journal of Prosthetics and Orthotics*, **21**, 91-96. https://doi.org/10.1097/JPO.0b013e3181a1ca54

[9] Wu, L., Carbone, G. and Ceccarelli, M. (2009) Designing an Underactuated Mechanism for a 1 Active DOF Finger Operation. *Mechanism and Machine Theory*, **44**, 336-348. https://doi.org/10.1016/j.mechmachtheory.2008.03.011

[10] Dalley, S.A., Bennett, D.A. and Goldfarb, M. (2014) Functional Assessment of the Vanderbilt Multigrasp Myoelectric Hand: A Continuing Case Study. *Proceedings of the* 2014 36*th Annual International Conference of the IEEE Engineering in Medi-*

cine and Biology Society (*EMBC*), Chicago, 6195-6198. https://doi.org/10.1109/EMBC.2014.6945044

[11] Choi, K.Y., Akhtar, A. and Bretl, T. (2017) A Compliant Four-Bar Linkage Mechanism that Makes the Fingers of a Prosthetic Hand More Impact R*esistant. Proceedings of the* 2017 *IEEE International Conference on Robotics and Automation*, Singapore, 6694-6699. https://doi.org/10.1109/ICRA.2017.7989791

[12] Resnik, L., Klinger, S.L. and Etter, K. (2014) The DEKA Arm: Its Features, Functionality, and Evolution during the Veterans Affairs Study to Optimize the DEKA Arm. *Prosthetics and Orthotics International*, **38**, 492-504. https://doi.org/10.1177/0309364613506913

[13] Ceccarelli, M. (2004) Fundamentals of Mechanics of Robotic Manipulation. Springer Science & Business Media, Berlin. https://doi.org/10.1007/978-1-4020-2110-7

[14] Li, G., Zhang, C., Zhang, W., Sun, Z. and Chen, Q. (2014) Coupled and Self-Adaptive Under-Actuated Finger with a Novel S-Coupled and Secondly Self-Adaptive Mechanism. *Journal of Mechanisms and Robotics*, **6**, 1-10. https://doi.org/10.1115/1.4027704

[15] Belzile, B. and Birglen, L. (2017) Optimal Design of Self-Adaptive Fingers for Proprioceptive Tactile Sensing. *Journal of Mechanisms and Robotics*, **9**, 1-11. https://doi.org/10.1115/1.4037113

[16] Yang, Y., Chen, Y., Wei, Y. and Li, Y. (2016) Novel Design and Three-Dimensional Printing of Variable Stiffness Robotic Grippers. *Journal of Mechanisms and Robotics*, **8**, 1-15. https://doi.org/10.1115/1.4033728

[17] Gogu, G. (2005) Chebychev-Grübler-Kutzbach's Criterion for Mobility Calculation of Multi-Loop Mechanisms Revisited via Theory of Linear Transformations. *European Journal of Mechanics—A/Solids*, **24**, 427-441. https://doi.org/10.1016/j.euromechsol.2004.12.003

[18] Dai, J.S., Huang, Z. and Lipkin, H. (2004) Mobility of Overconstrained Parallel Mechanisms. *Journal of Mechanical Design*, **128**, 220-229. https://doi.org/10.1115/1.1901708

[19] Chen, F.C., Appendino, S., Battezzato, A., Favetto, A., Mousavi, M. and Pescarmona, F. (2014) Human Finger Kinematics and Dynamics. New Advances in Mechanisms Transmissions and Applications, Springer, Berlin, 115-122. https://doi.org/10.1007/978-94-007-7485-8_15

[20] Hunt, K.H., Samuel, A.E. and McAree, P.R. (1991) Special Configurations of Multi-Finger Multi-Freedom Grippers-A Kinematic Study. *The International Journal of Robotics Research*, **10**, 123-134. https://doi.org/10.1177/027836499101000204

[21] Rocha, C., Tonetto, C. and Dias, A. (2011) A Comparison between the Denavit-Hartenberg and the Screw-Based Methods Used in Kinematic Modeling of Robot Manipulators. *Robotics and Computer-Integrated Manufacturing*, **27**, 723-728. https://doi.org/10.1016/j.rcim.2010.12.009

[22] Corke, P.I. (2007) A Simple and Systematic Approach to Assigning Denavit-Hartenberg Parameters. *IEEE Transactions on Robotics*, **23**, 590-594. https://doi.org/10.1109/TRO.2007.896765

[23] Singh, S., Singla, A., Singh, A., Soni, S. and Verma, S. (2016) Kinematic Modelling of a Five-DoFs Spatial Manipulator Used in Robot-Assisted Surgery. *Perspectives in Science*, **8**, 550-553. https://doi.org/10.1016/j.pisc.2016.06.017

[24] Dupuis, J., Holst, C. and Kuhlmann, H. (2017) Improving The Kinematic Calibration of a Coordinate Measuring Arm Using Configuration Analysis. *Precision Engineering*, **50**, 171-182. https://doi.org/10.1016/j.precisioneng.2017.05.004

[25] Du, Z., Yang, W. and Dong, W. (2015) Kinematics Modeling of a Notched Continuum Manipulator. *Journal of Mechanisms and Robotics*, **7**, 1-9. https://doi.org/10.1115/1.4028935

[26] Boscariol, P., Gasparetto, A., Scalera, L. and Vidoni, R. (2017) Efficient Closed-Form Solution of the Kinematics of a Tunnel Digging Machine. *Journal of Mechanisms and Robotics*, **9**, 1-13. https://doi.org/10.1115/1.4035797

[27] Li, J., Yu, L.D., Sun, J.Q. and Xia, H.J. (2013) A Kinematic Model for Parallel-Joint Coordinate Measuring Machine. *Journal of Mechanisms and Robotics*, **5**, 1-4. https://doi.org/10.1115/1.4025121

[28] Lipkin, H. (2005) A Note on Denavit-Hartenberg Notation in Robotics. *Proc. ASME International Design Engineering Technical Conferences and Computers and Information in Engineering Conference*, Long Beach, 24-28 September 2005, 921-926. https://doi.org/10.1115/DETC2005-85460

[29] Herath, H.M.C.M., Gopura, R.A.R.C. and Lalitharatne, T.D. (2017) Prosthetic Hand with a Linkage Finger Mechanism for Power Grasping Applications. *IEEE Life Sciences Conference*, Sydney, 304-307. https://doi.org/10.1109/LSC.2017.8268203

[30] Gopura, R.A.R.C., Bandara, D.S.V., Gunasekera, N.P.A., Hapuarachchi, V.H and Ariyarathna, B.S. (2017) A Prosthetic Hand with Self-Adaptive Fingers. 3*rd International Conference on Control, Automation and Robotics*, Nagoya, 269-274. https://doi.org/10.1109/ICCAR.2017.7942701

[31] Abeysekera, J. and Sha, H. (1987) Body Size Data of Sri Lankan Workers and Their Variability with Other Populations in the World: Its Impact on the Use of Imported Goods. *Journal of Human Ergology*, **16**, 193-208.

[32] Tomancak, P., Rueden, C. and Tinevez, J. (2007) Fiji ImageJ Open Source Java Image Processing Program. http://imagej.net